VOL. 8, NO. 10, OCTOBER 2013 ISSN 1819-6608
ARPN Journal of Engineering and Applied Sciences

www.arpnjournals.com

SIMULATION RESULTS ON EXPERIMENTAL IMPLEMENTATION OF CRONE CONTROL STRATEGIES FOR SPEED CONTROL OF A DC MOTOR

N. N. Praboo[1] and P. K. Bhaba[2]
[1]Department of Instrumentation Engineering, Annamalai University, Annamalai Nagar, India
[2]Department of Chemical Engineering, Annamalai University, Annamalai Nagar, India
E-Mail: praboonn@gmail.com

ABSTRACT

This work deals with the design of Commande Robuste d'Ordre Non Entier (CRONE) control strategy for the speed control of DC motor. The systematic design of three generations of CRONE control strategy is detailed. The transfer function of DC motor is derived analytically and represented as a second order model. Using this model the three generations of CRONE control strategies is designed and tested in simulation. The servo and regulatory responses of all the three generations of CRONE control strategy is compared and the result is reported in terms of error indices. The simulation results show that the third generation CRONE control strategy is more effective and gives superior performance over the other.

Keywords: DC motor, crone controller, non-integer order robust controller, integro-differentiation, black nichols locus.

1. INTRODUCTION

For the past several decades, many researchers contributed the findings towards the design and development of controllers. Most of the controllers designed are integer order and is developed from the time domain point of view. At the same time research activities towards the design of non-integer order and frequency domain based controllers was also given importance.

In this respect Manabe (1960) [1] introduced the concept of non-integer order [2, 3] integral controller based on the idea of having a constant phase margin around the gain crossover frequency (Bode's [4] ideal loop transfer function). Extending this idea, Oustaloup [5, 6] studied the fractional order control algorithms for the control of dynamic systems. Further he proposed a frequency domain based Commande Robuste d'Ordre Non Entier (CRONE) control strategy (1991).

The CRONE [7, 8, 9, 10] control system, the controller transfer function is defined using integro-differentiation with non-integer (fractional) order. By doing so, a flexible tuning and numerous choices of controller type is possible. Avoiding over estimation of plant disturbance leads CRONE to be a non-conservative robust control system. The control of continues and discrete time SISO and MIMO systems is also possible with CRONE strategy. The CRONE control strategy is classified into three generations are namely First, Second and Third CRONE controllers.

In this work, the three generations of CRONE control strategy is discussed. In this work, an attempt is made to evaluate the performance of first, second and third generation CRONE control strategies. The performance evaluation is carried out by implementing the three generations of CRONE controller to control the speed of DC motor. The implementation is done in MATLAB / Simulink platform assisted by CRONE Control System Design (CSD) toolbox [11, 12].

The paper is organized as follows: Section 2 provides the design methodology for the three different CRONE control generations. The obtaining of DC motor [13, 14] transfer function model using analytical approach is considered in Section 3. Section 4 deals with simulation results of all the three generations of CRONE controller. In section 5 controller performance results is discussed. Finally, the concluding remarks are given in Section 6.

2. CRONE CONTROL STRATEGY

2.1. First generation CRONE control strategy

The block diagram of first generation CRONE control system [7, 15] is shown in Figure-1, here e (t) is the input reference signal, y (t) is the plant output, u (t) is the controller output, dy (t) is the disturbances, G(s) is the plant transfer function, and C(s) is the CRONE controller.

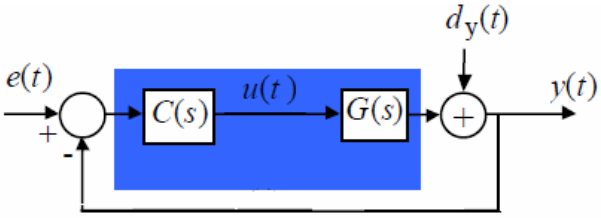

Figure-1. Block diagram of first generation CRONE control system.

The first generation CRONE controller is defined within a frequency range [ω_A, ω_B] around the desired open loop gain cross over frequency ω_{cg}. The ideal fractional order transfer function of first generation CRONE controller is defined as:

$$C(s) = C_0 s^n \text{, with } n \text{ and } C_0 \in \clubsuit \quad (1)$$

Here 'n' corresponds to fractional order integro - differentiator.

The Bode plot of first generation CRONE controller is shown in Figure-2. From the figure it is observed that the controller ensures a constant phase ($n\pi/2$) around the open loop gain crossover frequency ω_{cg}.

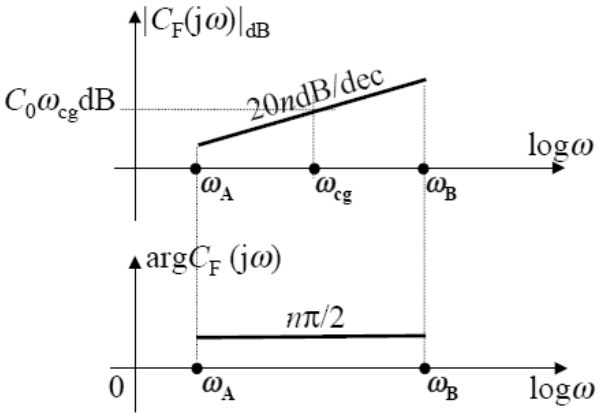

Figure-2. Bode plot of first generation CRONE controller.

The ideal fractional order transfer function C(s) can also be defined by a band-limited transfer function using corner frequencies ω_l and ω_h.

$$C(s) = C_0\left(\frac{1+s/\omega_l}{1+s/\omega_h}\right)^n, \ \omega_l \square \ \omega_A \text{ and } \omega_h \square \ \omega_B \quad (2)$$

The recursive distribution of real negative zeros and poles converts the fractional order band-limited transfer function into achievable rational order transfer function and is represented as:

$$C_R(s) = C_0 \prod_{i=1}^{N}\left(\frac{1+s/\omega'_i}{1+s/\omega_i}\right) \quad (3)$$

Where

$$\frac{\omega'_{i+1}}{\omega'_i} = \frac{\omega_{i+1}}{\omega_i} = \alpha\eta \quad \square\ 1 \quad (4)$$

$$\frac{\omega_i}{\omega'_i} = \alpha \quad and \quad \frac{\omega'_{i+1}}{\omega_i} = \eta \quad (5)$$

$$\alpha\eta = \left(\omega_h/\omega_l\right)^{1/N} \quad (6)$$

Where

$$\alpha = (\alpha\eta)^n \quad and \quad \eta = (\alpha\eta)^{1-n};$$
$$\omega'_1 = \omega_l \eta^{1/2} \quad and \quad \omega_N = \omega_h \eta^{-1/2} \quad (7)$$

To avoid phase undulations, it is convenient to choose a value of N which ensures a value of $\alpha\eta$ close to 5. To achieve desired control effort and to avoid steady state errors, the fractional (or) rational transfer function of first generation CRONE controller is cascaded with a band limited integrator of order n_I and a low pass filter of order n_F. After cascading, the complete fractional order first generation CRONE controller transfer function is given by:

$$C(s) = C_0\left(\frac{\omega_I}{s}+1\right)^{n_I}\left(\frac{1+s/\omega_i}{1+s/\omega_h}\right)^n \frac{1}{(1+s/\omega_F)^{n_F}} \quad (8)$$

Here the conditions $\omega_I \square \omega_l \square \omega_{cg} \square \omega_h \square \omega_F$ and the integer orders n_I and $n_F = 1$ must be satisfied to reject the input disturbance and to avoid the amplification of the high frequency measurement noise.

The robustness of the first generation CRONE controller is guaranteed only when the plant transfer function has a constant phase or atleast in a frequency range around the desired open loop gain crossover frequency ω_{cg}. Sometimes due to control effort limitations, it is impossible to select the desired open loop gain cross over frequency ω_{cg} within the asymptotic frequency band of the plant. This constraint made the author to develop the second generation CRONE controller.

2.2. Second generation CRONE control strategy

The block diagram of the second generation CRONE controller [8] is shown in Figure-3. In this strategy, a open loop fractional integrator transfer function $\beta(s)$ is introduced and it is represented as:

$$\beta(s) = C(s) * G(s) = \left(\frac{\omega_{cg}}{s}\right)^n, n \in [1,2] \quad (9)$$

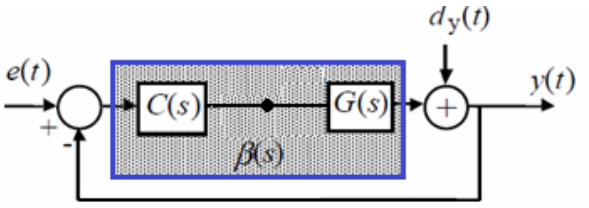

Figure-3. Block diagram of second generation CRONE controller.

The open loop fractional integrator transfer function $\beta(s)$ is plotted in black nichols plane within the frequency range [ω_A, ω_B] as shown in Figure-4. The nichols locus $\beta(s)$ forms a vertical straight line called frequency template, whose phase location is determined by order 'n' around the open loop gain crossover frequency ω_{cg}.

The change in plant parameters displaces the frequency template $\beta(s)$ vertically by providing a constant

phase around the desired open loop gain crossover frequency ω_{cg}. This ensures the robustness of second generation CRONE controller.

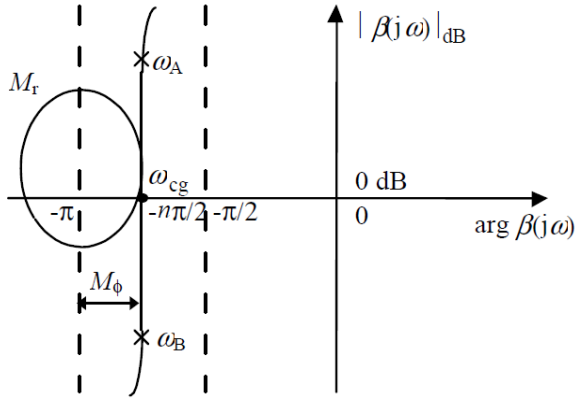

Figure-4. Nichols locus β(s) or Frequency template.

The complete open loop fractional integrator transfer function is represented as:

$$\beta(s) = K\left(\frac{\omega_I}{s}+1\right)^{n_I}\left(\frac{1+s/\omega_h}{1+s/\omega_l}\right)^{n}\frac{1}{(1+s/\omega_F)^{n_F}} \quad (10)$$

Where ω_I □ ω_l □ ω_{cg} □ ω_h □ ω_F. In addition, the integer orders n_I and n_F are selected based on the plant magnitude asymptotic behaviour at low and high frequencies.

The fractional order second generation CRONE controller C(s) is defined from the equation (9) and is represented as:

$$C(s) = \frac{\beta(s)}{G(s)} \quad (11)$$

The recursive distribution of poles and zeros of the complete open loop fractional integrator transfer function β(s) results in rational order open loop fractional integrator transfer function $\beta_R(s)$. From this the achievable rational order Second generation CRONE controller $C_R(s)$ is obtained as:

$$C_R(s) = \frac{\beta_R(s)}{G(s)} \quad (12)$$

Both the first and second generation CRONE controllers aim at being robust to plant gain variations. However other types of model uncertainty, like pole and zero misplacement are not taken into account. This motivated the author towards the development of third generation CRONE controller.

2.3. Third generation CRONE control strategy

The drawbacks of first and second generation CRONE controllers are overcome by the third generation CRONE controller [9] through handling of more general uncertainties than just gain-like perturbations. The design of third generation CRONE control strategy consists of different stages namely generalized template, optimal template and optimization of open loop behaviour.

2.3.1. Generalized template

The vertical straight line Nichols locus in the Nichols plane is previously defined in the second generation CRONE control strategy is replaced with any angle straight line segment called the generalized template shown in Figure-5. The generalized template is defined by a complex fractional order integration of fractional order n, whose real part determines its phase location at frequency ωcg, that is - $Re/_i$ (n) π/2 and whose imaginary part then determines its angle to the vertical.

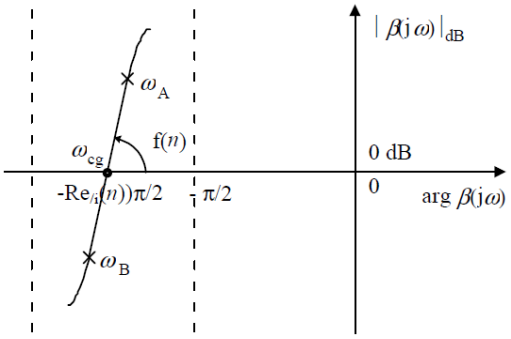

Figure-5. Generalized template in Nichols plane.

The complex fractional order integral transfer function is:

$$\beta(s) = \left(\cosh\left(b\frac{\pi}{2}\right)\right)^{sign(b)_I}\left(\frac{\omega_{cg}}{s}\right)^{a}\left(Re/_i\left((\omega_{cg})^{ib}\right)\right)^{-sign(b)} \quad (13)$$

With a+ib ∈ ¥$_i$ and s ∈ ¥$_j$,

Where are respectively time domain and frequency domain complex planes? Expanding the above equations provides.

$$\beta(s) = \left(\cosh\left(b\frac{\pi}{2}\right)\right)^{sign(b)_I}\left(\frac{\omega_{cg}}{s}\right)^{a}\left(\cos\left(b\ln\left(\frac{s}{\omega_{cg}}\right)\right)\right)^{-sign(b)} \quad (14)$$

From the derivatives of the β (jω) magnitude and phase at frequency ω_{cg}, the angle of the generalized template to the vertical can be expressed as a function of *a* and *b*:

$$\frac{d\left(|\beta(j\omega)|_{db}\right)}{d\left(phase\beta(j\omega)\right)} = \frac{-20asign(b)}{\ln(10)b\tanh(b\frac{\pi}{2})} \quad (15)$$

Where the transfer function of the generalized template is band-limited, then the equation is replaced by a more general expression.

$$\beta(s) = C^{sign(b)}\left(\frac{\omega l}{s}+1\right)^{n_l}\left(\alpha_0\frac{1+s/\omega h}{1+s/\omega l}\right)^{a} \times \left(\mathrm{Re}/_i\left(\alpha_0\frac{1+s/\omega h}{1+s/\omega l}\right)^{ib}\right)^{-qsign(b)}\left(\frac{1}{(1+\frac{s}{\omega h})^{n_h}}\right) \quad (16)$$

Where

$$C = \cosh\left(b\left(\tan^{-1}\left(\frac{\omega cg}{\omega l}\right)-\tan^{-1}\left(\frac{\omega cg}{\omega h}\right)\right)\right) \quad (17)$$

$$\alpha_0 = \left(1+\left(\frac{\omega_r}{\omega_l}\right)^2 / 1+\left(\frac{\omega_r}{\omega_h}\right)^2\right)^{1/2} \quad (18)$$

$$|b| \prec \min\left(\frac{\pi}{2\ln(\alpha_0)}, \frac{\pi}{2\left|\ln\left(\alpha_0\frac{\omega_h}{\omega_l}\right)\right|}\right) \quad (19)$$

Therefore the third generation fractional order CRONE cotroller is:

$$C(s) = \beta(s)/G(s) \quad (20)$$

2.3.2 Optimal template

The CRONE control strategy deals with the stability margins and performance, especially the closed loop resonant peak M_r in the Nichols magnitude contour (M-contour). Let M_{rd} be the resonant peak for the nominal plant G_o (jω). An indefinite number of open loop Nichols loci can tangent (Figure-6) the M-contour for the nominal parametric state of the plant. An optimal template is selected from these, if it tangents the M_{rd} M-contour around resonant frequency (ω_r) for the nominal plant state and if it minimizes the variations of the phase margin for the perturbed plant states.

The cost function minimized by the optimal template is described as:

$$J = M_{r\max} - M_{rd} \quad (21)$$

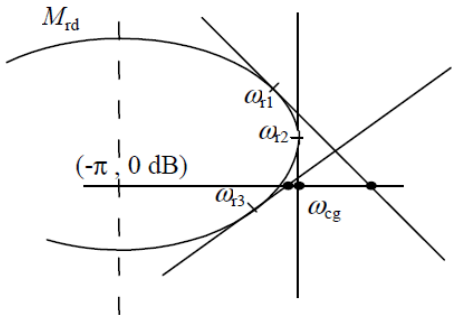

Figure-6. Infinite number of generalized template tangents.

The optimal template showed in Figure-7(b) positions the open - loop uncertainty domains correctly, so that they overlap the low stability margin areas as little as possible.

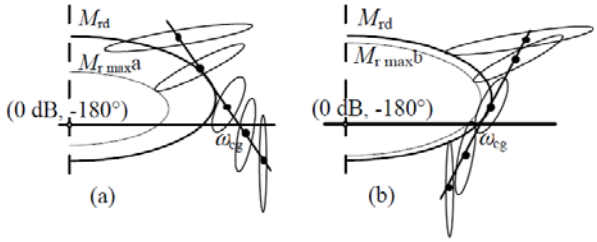

Figure-7. Generalized template Nichols loci and frequency uncertainty domains.

(a) Generalized template (GT) (b) Optimal template (OP)

GT: $M_{r\,max}{}^{a} - M_{rd} >>$ OT: $M_{r\,max}{}^{b} - M_{rd.}$

2.3.3. Optimization of the open-loop behaviour

There are eight high level parameters are there in open-loop transfer function β(s), they are n_l, n_h, a, b, ω_l, ω_h, ω_r and C. In which n_l and n_h are fixed by the control system designer. In order to obtain the tangency condition, ω_r and C are mentioned. A nonlinear optimization algorithm for the four independent parameters which minimises the cost function J based on the resonant peak variations and fulfils a set of shaping constraints on the four usual sensitivity functions T(S), S(s), CS(s) and GS(s). Synthesizing such a template through the optimization of three independent parameters (a tangency is imposed) from the four high-level parameters *a*, *b*, ω_l and ω_h, is the initial aim of the third generation Crone control.

The optimization of the generalized template consists in determining three optimal values from the following four parameters (Figure-8):

- Optimal real integration order *a*, which determines the position of the template along the axis 0 dB;
- Optimal imaginary integration order *b*, which then determines its angle to the vertical;

- Optimal corner frequencies ω_l and ω_h, which determine its length.

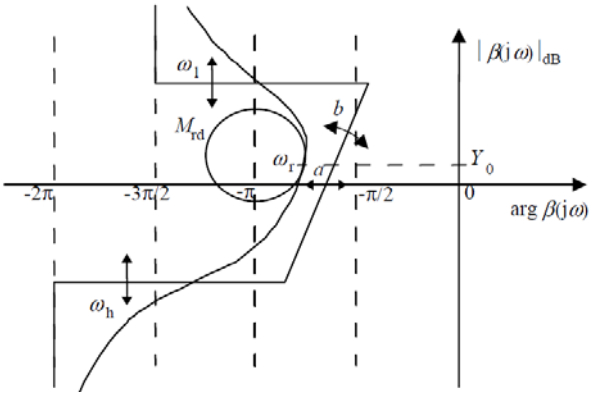

Figure-8. Effect of parameters a, b, ω_l and ω_h on the asymptotic Nichols locus.

The general form of third generation CRONE controller is given by:

$$C(s) = \beta(s)/G(s) \tag{22}$$

Where

$$\beta(s) = C^{sign(b)}\left(\frac{\omega l}{s}+1\right)^{n_l}\left(\alpha 0\frac{1+s/\omega h}{1+s/\omega l}\right)^{a} \times\left(\mathrm{Re}/i\left(\alpha 0\frac{1+s/\omega h}{1+s/\omega l}\right)^{ib}\right)^{-qsign(b)}\left(\frac{1}{(1+\frac{s}{\omega h})^{n_h}}\right) \tag{23}$$

The recursive distribution of real negative zeros and poles converts the fractional order band-limited transfer function into achievable rational order transfer function and is represented as:

$$C_R(s) = \beta_R(s)/G(s) \tag{24}$$

$$C_R(s) = \frac{C_0}{s^{N_{int}}}\frac{\prod_{i=1}^{n_1}1+\frac{s}{\omega_{zi}}}{\prod_{i=1}^{d_1}1+\frac{s}{\omega_{pi}}}\frac{\prod_{i=1}^{n_2}1+\frac{2\zeta_{zi}s}{\omega_{nzi}}+\frac{s^2}{\omega^2_{nzi}}}{\prod_{i=1}^{d_2}1+\frac{2\zeta_{pi}s}{\omega_{npi}}+\frac{s^2}{\omega^2_{npi}})} \tag{25}$$

Thus the design of third generation CRONE controller overcomes the limitations faced by the first and second generation CRONE controllers. In the following sections the mathematical modelling of DC motor is derived and performance of controllers is analysed.

3. SPEED CONTROL OF DC MOTOR

3.1. Process description

The DC motor is very popular in industry control area for a long time, since it shows high start torque characteristics compatible to most mechanical loads, high response performance, easier to be linear etc. This makes the motor controllable over a wide range of speeds. It can be considered as Single Input Single Output System (SISO). This paper focuses on the study of linear DC motor speed control. Therefore a separately excited DC motor is selected. The DC motor speed control setup [14] is shown in Figure-9. It consists of a separately excited DC motor with corrugated plate in the rotary shaft to transfer speed in the form of pulses. Opto-coupler is acting as sensor to measure the interval.

The DC motor speed is controlled by varying the armature voltage with the help of a chopper circuit since it is driven by PWM signals. The chopper circuit is used to convert the pulse width modulated signal from the PC through the card into the corresponding voltage. The V-MAT card is used to interface motor circuit with PC. It acts as a data acquisition card. Matlab® Simulink environment is used to monitor and control the speed of the motor from the PC.

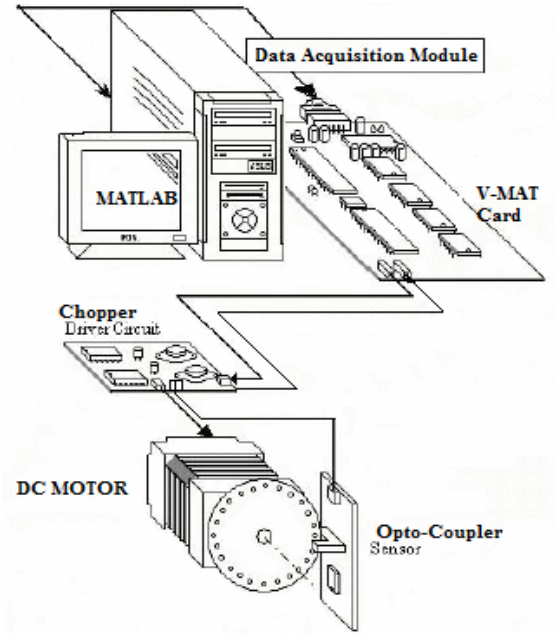

Figure-9. DC motor speed control system.

3.2. DC motor mathematical model

There are many methods of DC motor speed control exists, in this paper the speed of DC motor is controlled by varying the armature voltage of the motor coil. The armature voltage control method is purely based on some fixed parametric values like flux and field current in the control circuit. Thus the armature voltage controls the motor velocity. The control equivalent circuit of the DC motor by the armature voltage control method is

shown in Figure-10. The mathematical model is derived from the control circuit based on its input, output and inherent parameters of the DC motor.

Because the back EMF e_b is proportional to speed ω directly, then

$$e_b(t) = K_b \frac{d\theta(t)}{dt} = K_b \omega(t) \quad (26)$$

Making use of the KCL voltage law can get

$$e_a(t) = R_a i_a(t) + L_a \frac{di_a(t)}{dt} + e_b(t) \quad (27)$$

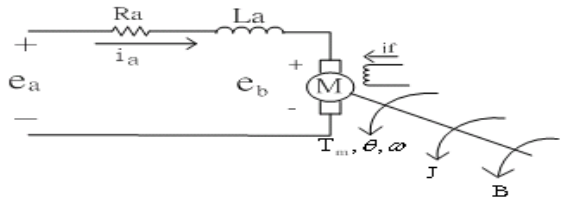

Figure-10. Control circuit of the DC motor using the armature voltage control.

R_a = armature resistance, L_a = armature inductance, i_a = armature current, i_f = field current
ω = angular velocity of motor, J = rotating inertial measurement of motor bearing.
e_a = input voltage, e_b = back electromotive force (EMF), T_m = motor torque, B = damping coefficient
From Newton law, the motor torque can obtain

$$T_m(t) = J \frac{d^2\theta(t)}{dt^2} + B \frac{d\theta}{dt} = K_T i_a(t) \quad (28)$$

Taking Laplace transform for the above given equations, the equation can be formulated as follows:

$$E_b(s) = K_b \omega(s) \quad (29)$$

$$E_a(s) = (R_a + L_a s) I_a(s) + E_b(s) \quad (30)$$

$$T_m(s) = Js\omega(s) + B\omega(s) = K_T i_a(s) \quad (31)$$

The following Figure-11 describes the DC motor armature control system functional block diagram.

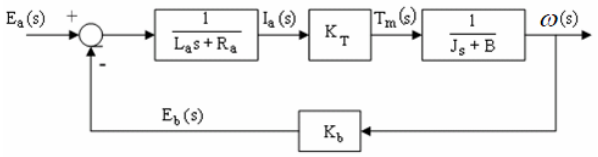

Figure-11. DC motor armature voltage control system functional block diagram.

The transfer function of DC motor speed with respect to the input voltage can be written as follows:

$$G(s) = \frac{\omega(s)}{E_a(s)} = \frac{K_T}{(L_a s + R_a)(Js + B) + K_b K_T} \quad (32)$$

3.3. DC motor speed control transfer function

The following table provides the DC motor control specification.

Table-1. DC Motor specifications

Moment of Inertia of the rotor	**J = 0.03 kgm^2**
Damping (friction) of the mechanical system	b =0.019 Nms
K_b=K_T=K	K =0.1331
Electric resistance	R = 6Ω
Electric inductance	L = 4.5 mH

On substituting the values of the control system parameters, the transfer function model is obtained as follows:

$$G(s) = \frac{\omega(s)}{E_a(s)} = \frac{1.01}{0.001025s^2 + 1.367s + 1} \quad (33)$$

4. CRONE CONTROLLER DESIGN

4.1. MATLAB and CRONE control toolbox

The simulation results of CRONE control strategy for speed control of DC motor are obtained using Simulink environment of MATLAB software. The CRONE CSD (Control System Design) Toolbox is designed by CRONE research group [12, 15].

4.2. First generation CRONE controller

First generation CRONE controller transfer function model is designed based on the DC motor plant transfer function (equation 33). The DC motor plant information is entered in the CRONE CSD toolbox for further computation. The DC motor plant perturbation is also considered. The perturbed gain changes are in the range of $0.08 < 1.01 < 1.2$.

The CRONE CSD toolbox is made of several commands like allowing, computing, visualizing and modifying the parameters of fractional and rational versions of CRONE controller. The Controller predefinition command allows setting the values of the parameters imposed by the user. The Controller predefinition parameters are listed in Table-2.

Table-2. CRONE Fractional controller parameter predefinition.

Required nominal open loop gain cross over frequency (ω_{cg})	**3**	**ω_A / ω_l ratio**	**10**
Required nominal phase margin P_m	54.9176	ω_h / ω_B ratio	10
Integral order n_i	1	ω_{AB} / ω_{cg} ratio	1
Low-pass filter order n_f	1	ω_{cg} / ω_i ratio	30
Fractional effect width ω_A / ω_B ratio	2.1535	ω_f / ω_{cg} ratio	30
Approx. Cell no	5	-	-

The computed first generation CRONE controller fractional values are listed in Table-3.

Table-3. First generation CRONE Fractional controller parameters.

Gain C_0	**17.0659**
Integral order n_i	1
Frequency ω_i (rad/sec)	0.1
Fractional order n	-0.52986
Fequency ω_l (rad/sec)	0.20847
Fequency ω_h (rad/sec)	43.1715
Low pass filter orde n_f	1
Filter Frequency ω_f (rad/sec)	90

According to the basic equation (8) for the first generation CRONE fractional controller, on substituting the values from Table-3, the controller takes the below given form.

$$C(s) = 17.0659\left(\frac{0.2087}{s}+1\right)^{1}\left(\frac{1+s/0.1}{1+s/43.1715}\right)^{-0.52986}\frac{1}{(1+s/90)^{1}} \quad (34)$$

Similarly on computing the values for the First generation CRONE rational controller are tabulated in Table-4.

Table-4. First generation CRONE rational controller parameters.

Gain C	**91.0195**
Cell number	5
Recursive factor η	1.6511
Recursive factor β	1.7597
Numerator corner frequencies ω_{ni} (rad/sec)	[0.1, 0.47139,1.3697, 3.9796, 11.5631, 33.5974]
Denominator corner frequencies ω_{ni} (rad/sec)	[0, 0.26788, 0.77833, 2.2615, 6.5709, 19.0923, 90]

Based on the rational values the controller is further synthesized as follows.

$$C_R(s) = 91.0195 \times \frac{(s+0.1)(s+0.47139)(s+1.3697)(s+3.9796)}{s(s+0.26788)(s+0.77833)(s+2.2615)} \times \frac{(s+11.5631)(s+33.5974)}{(s+6.5709)(s+19.0923)(s+90)} \quad (35)$$

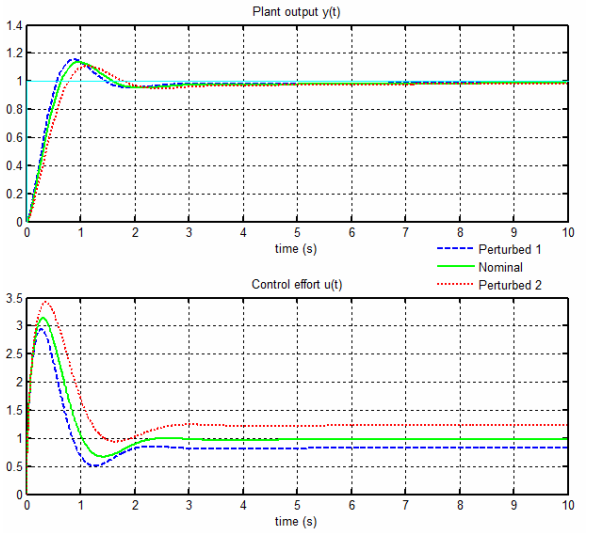

Figure-12. First generation CRONE controller unit step closed loop response with perturbations.

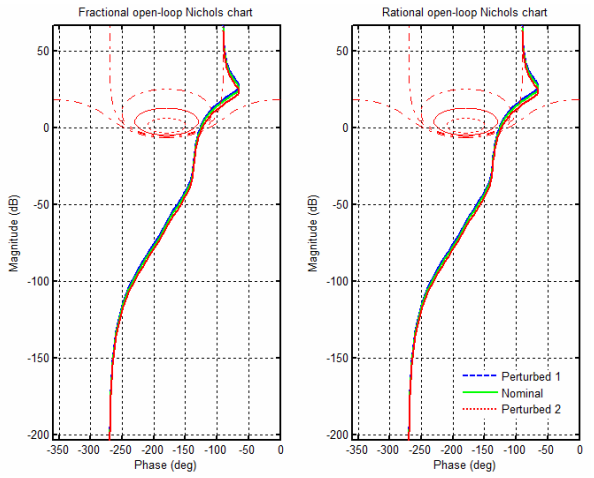

Figure-13. First generation CRONE fractional and rational open loop Nichols chart.

4.3. Simulation of second generation CRONE control strategy

On following the general initial procedures of CRONE control strategy, which is already discussed in simulation of First generation CRONE controller. The Second generation CRONE fractional parameters are evaluated and tabulated in Table-5.

Table-5. Second generation CRONE fractional controller parameters.

Gain K	**34.9238**
Low frequency order n_l	1
High frequency order n_h	3
Fractional order n	1.3307
Fequency ω_l (rad/sec)	0.20847
Fequency ω_h (rad/sec)	43.1715
Fractional effect width ω_A / ω_B	2.0709
ω_A / ω_l ratio	10
ω_h / ω_B ratio	10

Substituting the given values in equation 16, the open loop fractional transfer function is obtained as:

$$\beta(s) = 34.9238 \left(\frac{0.20847}{s}+1\right)^{1}\left(\frac{1+s/43.1715}{1+s/0.20847}\right)^{1.3307}\frac{1}{(1+s/43.1715)^{3}} \quad (36)$$

The rational controller parameters are computed and shown in Table-6.

Table-6. Second generation CRONE rational controller parameters.

Gain C	**28.787**
Cell number	5
Recursive factor η	1.423
Recursive factor β	2.0419
Numerator corner frequencies ω_{ni} (rad/sec)	[0.4239, 0.73649,1.2316, 3.5786, 10.3979, 30.2118]
Denominator corner frequencies ω_{ni} (rad/sec)	[0, 0.2979, 0.8655,2.5149, 7.3073,21.2318,43.17]

Based on the above parameters the Second generation CRONE controller rational transfer function is obtained as:

$$C_R(s) = 28.787 \times \frac{(s+0.423)(s+0.73649)(s+1.2316)}{s(s+0.2979)(s+0.8655)(s+2.5149)} \times \frac{(s+3.5786)(s+103979)(s+30.2118)}{(s+7.3073)(s+21.2318)(s+43.17)} \quad (37)$$

Unit step response of the second generation CRONE controller with perturbation is shown in Figure-14 and the Nichols chart of second generation CRONE fractional and rational open loop is shown in Figure-15.

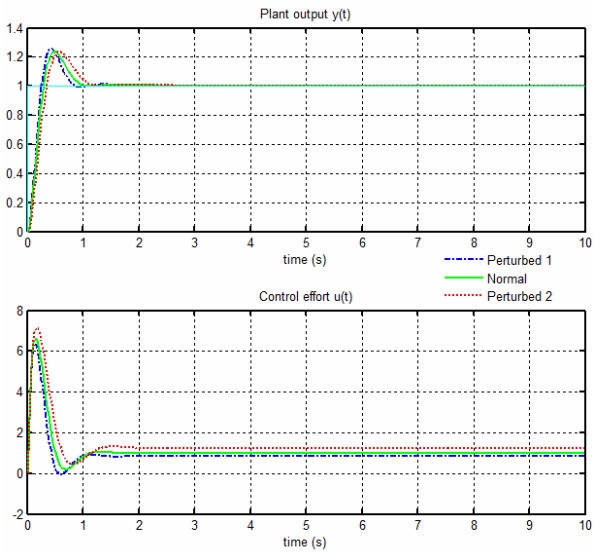

Figure-14. Second generation CRONE controller unit step closed loop response with perturbations.

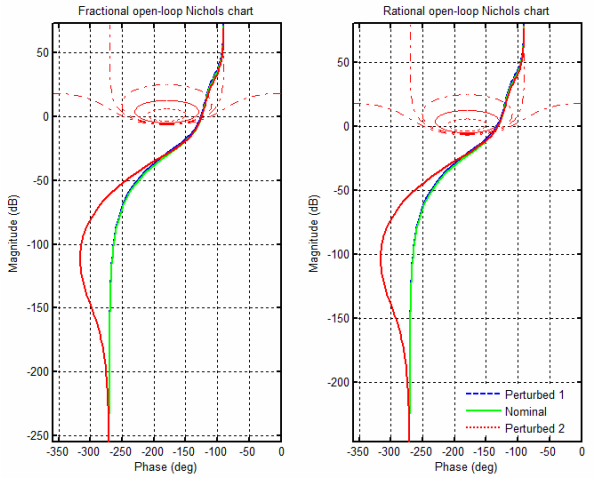

Figure-15. Second generations CRONE fractional and rational open loop Nichols chart.

4.4. Third generation crone control strategy

Similar to that of First and Second generation CRONE controllers, the plant parameters, time domain and frequency domain specifications are entered into the CRONE CSD Toolbox and following the design procedures one can obtain the third generation fractional optimized open loop transfer function parameters is shown in Table-7.

Table-7. Third generation CRONE open loop parameters.

C	9.78243	magnitude Y_o	2
n_l	1	Phase x_o	-127.236
n_h	3	a	1.21693
ω_l	0.6	b	0.278608
ω_h	15	q	1
ω_r	3	α_0	5

Substituting the given values in equation 23, the open loop fractional optimized transfer function is obtained as:

$$\beta(s)=9.78243^{sign(0.278608)}\left(\frac{0.6}{s}+1\right)^{1}\times\left(5\frac{1+s/15}{1+s/0.6}\right)^{1.21693}\times\left(\mathrm{Re}/i\left(5\frac{1+s/15}{1+s/0.6}\right)^{i0.278608}\right)^{-1sign(0.278608)}\times\left(\frac{1}{(1+\frac{s}{15})^{3}}\right) \quad (38)$$

The rational optimized CRONE controller parameters are shown in Table-8.

Table-8. Rational optimized CRONE controller parameters.

Gain	**5.01187**			
Integration order	**1**			
Zeros				
Corner frequencies	ω_1	1710	ω_2	0.555
Order	o_1	1	o_2	1
Damping constant	d_1	1	d_2	1
Poles				
Corner frequencies	ω_1	18.3	ω_2	18.3
Order	o_1	1	o_2	1
Damping constant	d_1	1	d_2	1

On substituting the above given parameters in equation, the rational optimized CRONE controller transfer function is given below:

$$C_R(s)=\frac{5.00187}{s}\frac{(1+\frac{s}{1710})}{1+\frac{s}{18.3}}\frac{(1+\frac{2s}{1710}+\frac{s^2}{(1710)^2})}{(1+\frac{2s}{18.3}+\frac{s^2}{(18.3)^2})}\times\frac{(1+\frac{2s}{0.555}+\frac{s^2}{(0.555)^2})}{(1+\frac{2s}{18.3}+\frac{s^2}{(18.3)^2})} \quad (39)$$

Unit step response of the third generation CRONE controller with perturbation is shown in Figure-16 and the Nichols chart of second generation CRONE fractional and rational open loop is shown in Figure-17.

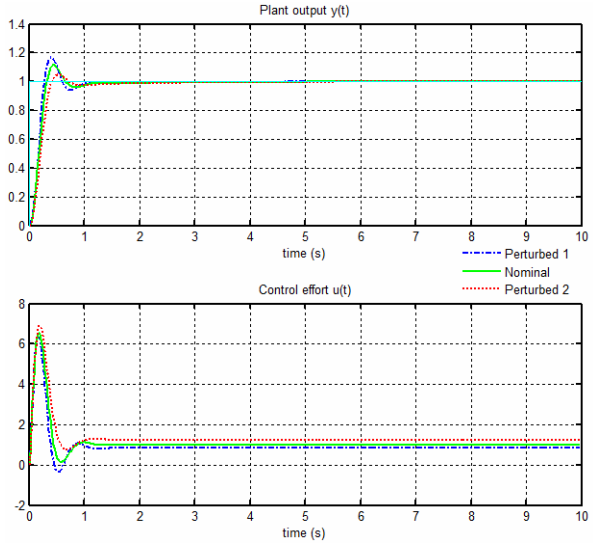

Figure-16. Third generation CRONE controller unit step closed loop response with perturbations.

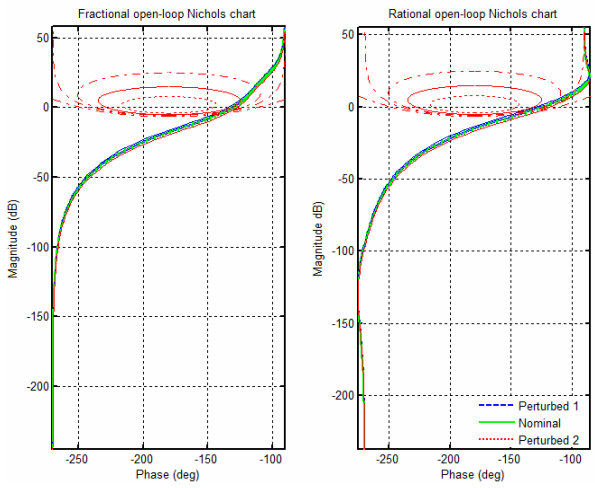

Figure-17. Third generation CRONE fractional and rational open loop Nichols chart.

5. RESULTS AND DISCUSSIONS

The performance of set-point tracking for the three generation CRONE control strategies for the speed control of DC motor are compared based on ISE and IAE error indices. The servo response is made at 50% (i.e., 750 rpm) set point of speed. Different step changes are applied at ±5%, ±10% and ±15%. The performances are tabulated in Table-9. The servo responses for the three generations of CRONE controllers are shown in Figure-18.

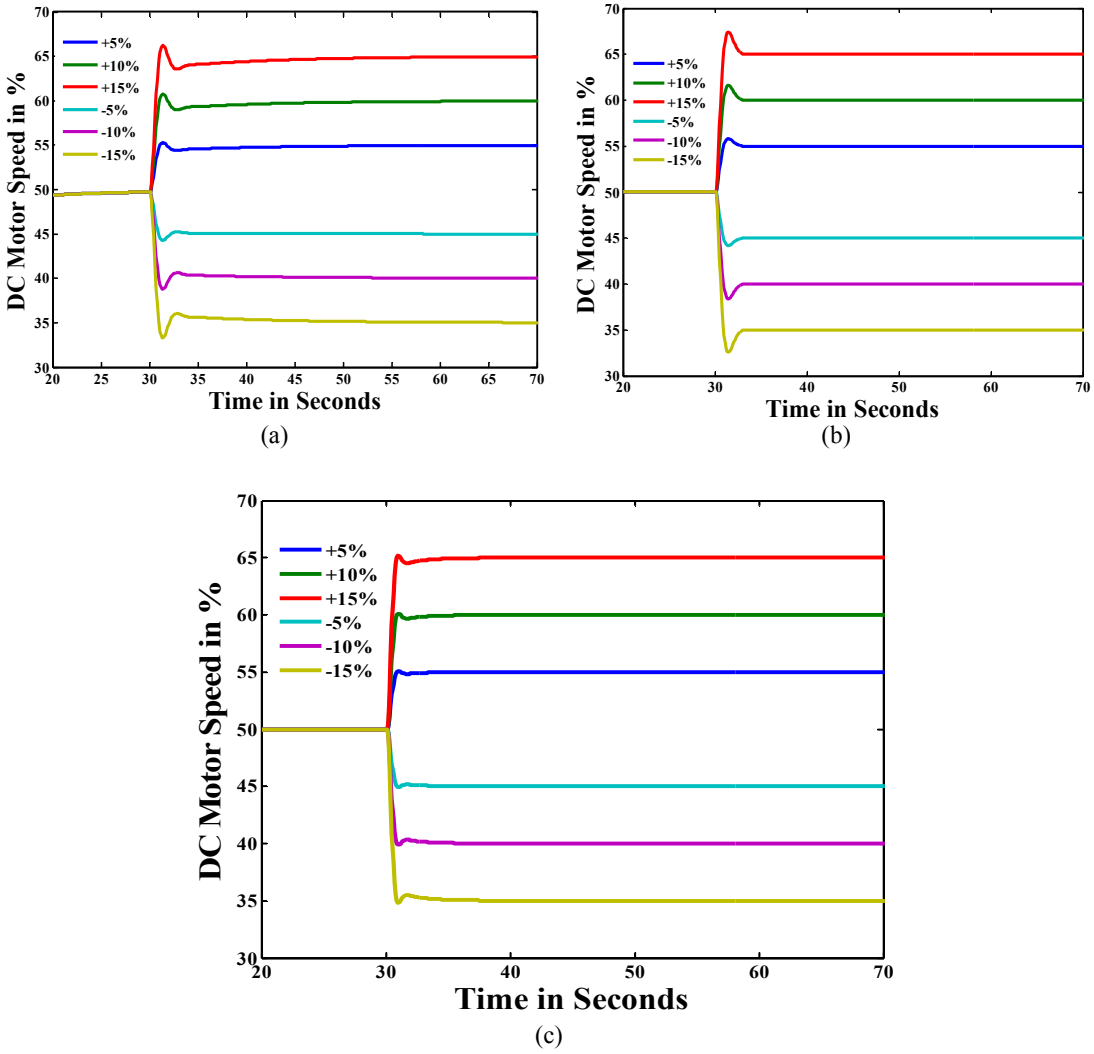

Figure-18. Servo response of speed control of DC motor using (a) First generation (b) Second generation and (c) Third generation CRONE controllers.

Table-9. Performance measures in terms of ISE and IAE at operating point 50% of the DC motor speed.

Set point tracking cases	First generation crone		Second generation crone		Third generation crone	
	ISE	IAE	ISE	IAE	ISE	IAE
+15%	84.2	19.7	82.15	10.9	59.32	5.23
+10%	39.14	13.8	37.7	7.22	26.36	4.45
+5%	10.35	7.8	9.13	3.55	6.591	2.02
-5%	10.33	6.8	9.126	3.47	6.592	2.11
-10%	39.1	11.7	37.6	7.43	26.38	4.01
-15%	84	17.8	82.16	11.24	59.33	5.11

Table-10. Performance measures in terms of ISE and IAE at operating point 50% of the DC motor speed with load change of 2%.

Load tracking (2% load change)	**First generation crone**	**Second generation crone**	**Third generation crone**
ISE	1.568	1.503	1.066
IAE	2.505	1.311	0.8586

The load tracking performance of the three generation CRONE control strategies for the speed control of DC motor are compared based on ISE and IAE error indices. The regulatory response is made at 50% (i.e., 750 rpm) set point of speed with load disturbance of 2%. The integral performance indices IAE and ISE for the regulatory response is tabulated in Table-10.

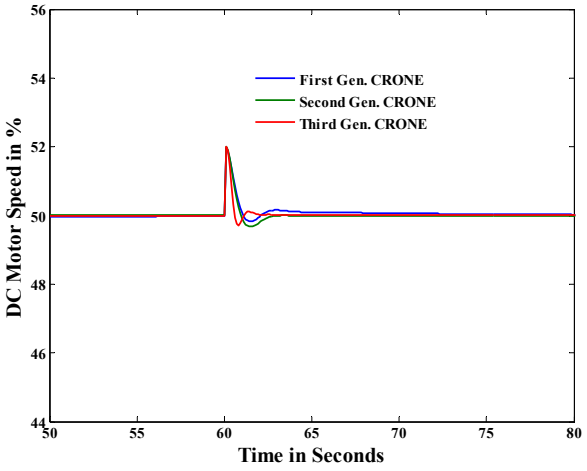

Figure-19. Regulatory response of speed control of DC motor using all Gen. CRONE controllers with 2% load change at 50% (750 rpm) of speed.

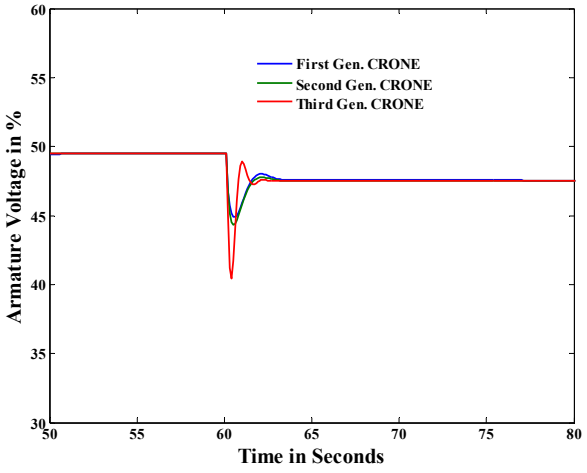

Figure-20. Controller output of all Gen. CRONE controller with 2% load change at 50% (750 rpm) of speed.

6. CONCLUSIONS

In this paper the design of three generation CRONE control strategy is discussed. From the design, it is inferred that the limitations of first generation CRONE controller are overcome by providing a constant phase by displacing frequency template corresponding to the parametric changes. Similarly the draw back of second generation CRONE control strategy is overcome by any angle straight line generalised template, thereby handling more general uncertainties.

The three generation CRONE controller is designed for the speed control of DC motor by varying the armature voltage of the motor. The CRONE controller design is performed using CRONE control system design tool box developed by CRONE research group. The servo and regulatory responses of the system is recorded and its performance is analysed using ISE and IAE criteria. It is inferred that the third generation CRONE controller outperforms other generation of controllers. The second generation CRONE controller performs better than the first generation CRONE controller.

REFERENCES

[1] S. Manabe. 1960. The non-integer integral and its application to control systems. Japanese institute of electrical engineers journal. 80(860): 589-597.

[2] I. Podlubny. 1999. Fractional Order systems and PID-controllers, in IEEE transaction on Automatic Control. 44(1): 208-214.

[3] N. N. Praboo, P K. bhaba and S.E. Hamamci. 2010. Fractional Order Pi^{λ} control strategy for a Liquid level system. IEEE proceedings of world congress on Nature and Biologically Inspired Computing, Kitakyushu, Japan. pp. 121-126.

[4] H.W. Bode. 1945. Network Analysis and Feedback Amplifier design. New York: van Nostrand, NY, USA.

[5] A. Oustaloup. 1991. La commande CRONE, Editions HERMES, Paris.

[6] A. Oustaloup, X. Moreau and M. Nouillant. 1996. The CRONE suspension. Control engineering Practice. 4(8): 1101-1108.

[7] A. Oustaloup and M. Bansard. 1993. First generation CRONE controls. IEEE international conference on systems, man and cybernetics - Le Touquet, 17-20, October, France.

[8] A. Oustaloup, B. Mathieu and P. lanusee. 1993. Second generation CRONE control. IEEE international conference on systems, man and cybernetics - Le Touquet. 17-20 October, France. pp. 136-142.

[9] A. Oustaloup, B. Mathieu and P. lanusee. 1993. Third generation CRONE control. IEEE international conference on systems, man and cybernetics - Le Touquet. 17-20 October, France. pp. 149-155.

[10] A. Oustaloup, B. Mathieu and P. lanusee. 1993. The Great principles of the CRONE control. IEEE international conference on systems, man and cybernetics - Le Touquet. 17-20 October, France. pp. 118-129.

[11] A. Oustaloup, P. Melchior, P. Lanusse, O. Cois and F. Dancla. 2000. The CRONE tool box for MATLAB, IEEE international symposium on Computer aided control system. Design, Anchorage, Alaska, USA, September 25-27.

[12] CRONE tool box, CRONE research group, Universite de Bordeaux, France.

[13] Baek S. M. and T. Y. Kuc. 1997. An adaptive PID learning control of DC motor. IEEE International. 3: 2877-2882.

[14] Guoshing Huang and Shuocheng Lee. 2008. PC-based PID Speed Control in DC Motor. IEEE, ICALIP.

[15] A. Monje, Yang Quan Chen, Blas M. Vinagree, Dingyu xue and Vicente Feliu. 2010. Fractional Order systems and controls: Fundamentals and applications, Advances in industrial control, Springer.